Russian Chemical Reviews

August 1988

Translated from *Uspekhi Khimii*, **57**, 1233-1252 (1988)

U.D.C. 539.26:549.641 + 546.655

The Influence of Surface Microstructures on the Physicochemical Properties of Oxides

A.I.Leonov, Yu.P.Kostikov, and V.S.Strykanov

Published data on the role of defects and the microstructures formed on them in the chemistry of solid oxides have been examined. The conditions of formation, stability, and breakdown of the microstructures obtained on the external surface, at the phase boundaries, and in the inter-crystallite layers in polycrystalline solids have been described. It has been shown that surface compounds have an activating and an inhibiting action on the kinetics of solid-phase chemical reactions and on the thermomechanical and electrophysical properties of oxide materials.
The bibliography contains 74 references.

CONTENTS

I. Introduction 705
II. Methods for studying the surface and the inter-phase boundaries 706
III. The formation of the microstructures on defects in oxides containing an impurity, and their properties 707
IV. The relationship between the change in the defect character and the sequence of chemical reactions in mixtures of solid oxides 710
V. The mechanism of the action of impurities in sintering, and the deformational properties and thermal stability of oxide materials 712
VI. Surface microstructures and the protection of ceramic materials from reduction 714
VII. The influence of surface structures on the electrical properties of ceramic materials 714

I. INTRODUCTION

The study of surface microstructures is becoming one of the principal research fields in solid state chemistry and physics. All heterogeneous catalytic reactions take place on a surface, and progress in heterogeneous catalysis depends on the study of the composition, structure, and energetics of surface microstructures. The properties of metallic and non-metallic constructional materials are determined to a large extent by the phase boundaries and the grain boundaries, which are the most important structural elements. The study of the influence of defect microstructures (dislocations, grain boundaries, and phase boundaries) on the electronic processes in semiconductors is extremely important. Surface structures have an extremely marked influence on the kinetics of crystal growth and the habit and degree of perfection of crystals.

In the present review, published data on the role of surface microstructures in the physical chemistry of oxides have been systematised, and a critical analysis has been carried out. The dependence of the

properties of microstructures on the chemical character and concentration of impurities and on temperature, and the formation of non-equilibrium (intermediate) compounds in solid-phase chemical reactions as a consequence of the defect character of the structure, have been examined. Data on the influence of microstructures on the kinetics of the sintering of ceramic masses, the deformation of materials at high temperatures, and the electrophysical properties of doped oxides have been discussed.

II. METHODS FOR STUDYING THE SURFACE AND THE INTER-PHASE BOUNDARIES

Widely employed methods of analysis—chemical analysis, X-ray diffraction, spectroscopy, microscopy— do not give the required information on the properties of a surface and micro-volumes. The present section gives brief characteristics of some of the most informative methods for the analysis of a surface, the grain boundaries, and the phase boundaries in ceramic materials.

1. *X-Ray spectral microanalysis (XMA)* is based on the study of the X-ray emission spectra; the emission is excited in the specimen being analysed by an electron probe with a diameter of $0.7-1$ μm on the surface of the specimen. XMA can be used to determine all the elements from Li onward; the sensitivity is ~ 1 at.% for the light elements, and ~ 0.1 at.% for the middle and heavy elements. The spatial resolution is $1-3$ μm, because of the scattering of the exciting electron beam in the massive specimen. The thickness of the specimen is much greater than the mean free path of the electrons with an energy of $5-20$ keV usually employed in XMA.[1]

XMA can be used to carry out the local (within $1-3$ μm) qualitative and quantitative analysis of a substance with an accuracy of ~ 2 rel.%, to study the distribution of elements over the surface of a specimen, to study the reaction at a phase boundary, and to determine diffusion characteristics.

For XMA, the specimen should have a well polished surface, in order to observed its microstructure in a metallographic microscope and, which is more important, in order to carry out quantitative analysis, since the surface relief influences the intensity of the X-ray emission recorded. There are no restrictions on the electrophysical characteristics of the specimens.

2. *Scanning electron microscopy* makes it possible to study the topography of the surface of a specimen, its microstructure, and its domain structure in the case of ferromagnetics and ferroelectrics. When the back-reflected scattered electrons are recorded, the image produced gives information on the distribution of the elements on the surface of the specimen, particularly if the atomic number of the element concentrated at the grain boundaries differs considerably from that of the basic compound.[2] The attainable resolution is 10 nm.[3] The scanning electron microscope gives a resolution of ~ 1 μm when operating under X-ray microanalysis conditions.

3. *Scanning transmission electron microscopy (STEM)* can be used to study the microstructure and the morphology of the intergranular formations, and to determine the structure of phases by microdiffraction. The attainable spatial resolution is $\sim 3-5$ nm. A characteristic of STEM is that it is possible to carry out routine microanalysis with a spatial resolution of ~ 20 nm.[4,5] This high resolution is made possible by the use of electron beams with a field emission cathode, which make it possible to obtain an electron probe with a diameter $\leqslant 10$ nm on the surface of a specimen. Since STEM uses specimens whose thickness ($150-650$ nm) is smaller than the mean free path of the electrons in the specimen, the broadening of the beam in the specimen as a result of scattering is slight, and the diameter of the region analysed is $2-3$ times the diameter of the probe on the surface of the specimen.[6] The broadening also depends on the thickness of the specimen, the energy of the electron probe, and the characteristics of the target—atomic number, atomic mass, and density. Quantitative X-ray spectral analysis is difficult, so that the results of microanalysis by STEM must be regarded as only a qualitative demonstration of enrichment of the grain boundary.[5]

The preparation of specimens for STEM is tedious and complicated, since it is necessary to reduce the thickness of the specimen to ~ 100 nm. Chemical etching and etching by ion bombardment are used for this purpose. The preparation of the specimens may have a significant influence on the results, since in chemical etching, selective etching of different phases may take place, and in etching by ion bombardment, the atomisation of different elements is irregular[3] and the temperature of the specimen increases considerably, so that chemical reactions may take place with a change in the phase composition of the specimen. This must be borne in mind when discussing the results of microanalysis by STEM.

4. *Auger electron spectroscopy (AES)* is based on the analysis of the Auger electrons emitted by the specimen when it is irradiated by a beam of electrons with an energy of $1-3$ keV. The depth of removal of the Auger electrons varies from 0.4 nm to 3 nm, depending on their kinetic energy.[3] The AES data therefore carry information on the surface layer of the specimen.

AES makes it possible to determine the qualitative and approximate quantitative composition of the surface (all elements except H and He); its sensitivity corresponds to $\sim 10^{-2}$ monolayer. Under scanning conditions it is possible to study the distribution of the elements over the surface of the specimen; the spatial resolution in this case is determined by the diameter of the exciting beam of electrons, and is usually $5-20$ μm. The most interesting feature is the possibility of observing the Auger spectra directly during the ion etching of the specimen; this makes it possible to obtain the distribution of elements along the depth and to obtain information on the reactions taking place in the region of a phase interface. No special preparation of the specimens is required; in the study of dielectrics, difficulties are encountered, associated with the charging of the surface.

5. *X-Ray photoelectron spectroscopy (XPES)* or electron spectroscopy for chemical analysis (ESCA) is based on the analysis of the photoelectrons emitted by the specimen when it is irradiated by a monochromatic beam of X-rays. The depth of removal of the photoelectrons is several nanometres, that is spatial ESCA, like AES, carries information about the surface of the specimen. XPES has no spatial resolution over the surface, since it is extremely difficult to focus the X-ray beam to a diameter smaller than 1 mm.

XPES makes it possible to carry out the qualitative and quantitative analysis of a surface and to determine all the elements of the periodic system with a sensitivity of ~ 0.1 at.% (for uniform distribution of the element being determined) and an uncertainty of not more than 10 rel.%.

A significant advantage of XPES is the simplicity of quantitative analysis, since there is no inter-element influence in the determination of any elements. Special preparation of the specimens is not required, and there are no restrictions on the electrophysical properties of the specimens. The methods are more informative when XPES and AES are used together.

6. *Secondary ion mass spectroscopy (SIMS)* is based on the analysis of the secondary ions emitted by a target when it is bombarded by a beam of primary ions with an energy of 1–20 keV. The secondary ion mass spectrum contains differently charged monatomic ions of the main substance, the ions of polyatomic clusters, and the ions of impurities and chemical compounds, and the interpretation of the mass spectrum is tedious. A significant advantage of SIMS over other methods is its high sensitivity, from 10^{-7} at.% to 10^{-9} at.%.

The recording of the mass spectra with constant etching of the surface of the specimen makes it possible to obtain the distribution of the elements being determined along the thickness of the surface layer; the resolution along the layer (with allowance for the physical factors restricting the resolution—the roughness of the surface, the formation of etching facets or cones, and atomic mixing) is ~10 nm.

In the ion micro-probe, in the study of the distribution of elements over the surface of the specimen, the spatial resolution is determined by the size of the ion probe (1–10 μm). Preliminary preparation of the specimens is not required. The analysis of dielectrics is difficult, because of charging of the surface.

7. *Autoradiography (ARG)* is based on the recording of the distribution of a radioactive isotope in the specimen being studied from the blackening of photoemulsion applied to the specimen (or a photographic plate), under the influence of nuclear radiation. For contact radiography, the spatial resolution is ~20 μm, and for radiography with applied emulsions combined with electron microscopy the resolution is ~1 μm. ARG gives information on the diffusion characteristics of the phase boundaries and grain boundaries.[7] Any material can be studied by autoradiography. The restrictions are related to the selection of a radioactive isotope of the element being studied, suitable for radiography.

A detailed comparative analysis of methods for studying a surface has been given in a published review.[8]

III. THE FORMATION OF THE MICROSTRUCTURES ON DEFECTS IN OXIDES CONTAINING AN IMPURITY, AND THEIR PROPERTIES

Natural minerals and oxides used in technology contain non-controlled impurities or specially intoduced additives (mineralisers, activators, modifiers), which form microstructures as a result of internal adsorption on defects. Table 1 gives the compositions of microstructures in oxides, determined by XPES and using electron and ion micro-probes.

X-Ray electron studies of polycrystalline oxides[9] containing small quantities of impurity (0.01–1 mole %) showed that in the specimens $MgO-[Al_2O_3]$, $SnO_2-[CaO]$, $TiO_2-[CaO]$, and $TiO_2-[BaO]$, the compounds $MgAl_2O_4$,[9–12] $CaSnO_3$,[14] $CaTiO_3$, and $BaTiO_3$ [9] respectively are formed as local microstructures in the region of the defects. The synthesis temperature was 1650–1800 K. The composition of the surface was determined from the integral intensity of the analytical lines $Mg2s_{1/2}$, $Ca2p_{3/2}$, $Ba3d_{5/2}$, $Al2s_{1/2}$, $Ti2p_{3/2}$, and $Sn3d_{5/2}$ with allowance for the photo-ionisation cross-sections.[27]

The results of an X-ray electron study of the polycrystalline oxide MgO containing small quantities of added Al_2O_3 are given in Fig.1.[10] With increase in the Al_2O_3 concentration from 0.4 mole % to 2 mole % in the surface layer there was a decrease in the concentration of Mg in octahedral coordinatoin [binding energy E_b(Mg. $2s_{1/2}$) = 87.5 eV], indicating the formation of spinel $MgAl_2O_4$.

Table 1. The formation of microstructures on defects containing impurities (0.01–1 mole %).

Oxide	Impurity	Microstructure	Refs.
MgO	Al_2O_3	$MgAl_2O_4$	[9–11]
Al_2O_3	MgO	$MgAl_2O_4$	[12]
Al_2O_3	$Ln_2O_3^*$	$LnAlO_3$	[13]
SnO_2	CaO	$CaSnO_3$	[9, 14]
SnO_2	TiO_2	TiO_2 in SnO_2**	[9, 15]
SnO_2	ZnO	ZnO in SnO_2**	[9, 16]
SnO_2	NiO	NiO in SnO_2**	[9, 16]
SnO_2	Nb_2O_5	Nb_2O_5 in SnO_2**	[9, 16]
ZrO_2	CaO	$CaZrO_3$, $CaZr_4O_9$	[9, 17, 18]
ZrO_2	Y_2O_3	Y_2O_3 in ZrO_2**	[9, 19]
Al_2O_3	NiO	$NiAl_2O_4$	[9, 12]
Cr_2O_3	CrO_3	$xCr_2^{III}O_3 \cdot yCr^{VI}O_3$	[9, 20, 21]
Cr_2O_3	La_2O_3	$La_2(CrO_4)_3$	[9, 20, 22]
MgO	NiO	NiO in MgO**	[9]
TiO_2	SnO_2	SnO_2 in TiO_2**	[15]
SnO_2	SiO_2	eutectic	[15]
Nb_2O_5	BaO	$BaNb_6O_{16}$ in Nb_2O_5**	[23]
Ta_2O_5	Nb_2O_5	Nb_2O_5 in Ta_2O_5**	[23]
$BaTiO_3$	$SrTiO_3$	$SrTiO_3$ in $BaTiO_3$**	[23]
$CaTiO_3$	CaO	Ca_3TiO_5	[24]
TiO_2	Ta_2O_5	$TiTaO_4$ in TiO_2**	[25]
CoO	Cr_2O_3	$CoCr_2O_4$	[26]
CeO_2	La_2O_3	$mLa_2O_3 \cdot nCeO_{2-x}$	[10]
TiO_2	CaO	$CaTiO_3$	[9]
TiO_2	BaO	$BaTiO_3$	[9]
Al_2O_3	Y_2O_3	$Y_4Al_2O_9$, $YAlO_3$	[9]

*Ln = La, Ce, Pr, Nd.
**Solid solutions.

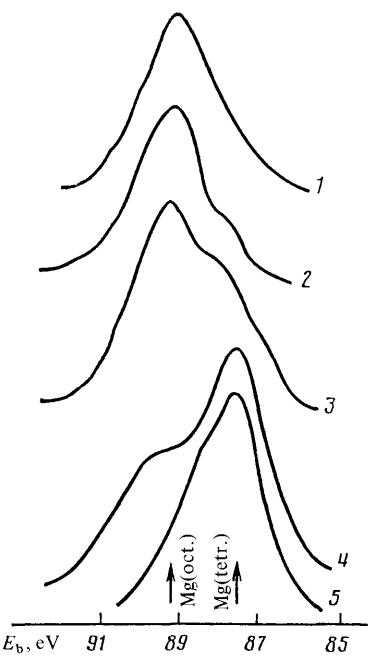


Figure 1. Mg2*s* X-ray electron spectra: *1*) MgO, *2–4*) MgO containing 0.4, 0.8, and 2.0 mole % Al_2O_3 respectively, *5*) $MgAl_2O_4$ (spinel).[10]

The ratio Al/Mg in the surface layer with a thickness of ~8.0 nm, found from the intensities of the Mg and Al lines, is 0.3, whereas in spinel, Al/Mg = 2. This lack of agreement is apparently due to the formation of spinel as local inclusions in an MgO matrix both along the depth of the layer and over the surface of the specimen, and the observed value of the Al/Mg ratio is the averaged value. Electron-microscope studies[11] showed that the formation of spinel involves the accumulation of crystals with dimensions of 0.5–10 μm, distributed in disordered fashion in the surface layer.

The dependence of the surface formations in a CeO_2 ceramic on the concentration of added La_2O_3 has been studied experimentally.[10] The $Ce3d_{5/2}$ spectrum in CeO_2 has characteristic lines with E_b = 882.3 eV and E_b = 882.6 eV. When CeO_2 contains added La_2O_3, a new $Ce3d_{5/2}$ line appears, with E_b = 381.3 eV, which can be assigned to a surface compound. The enrichment in La_2O_3 of a surface layer with a thickness of 8–10 nm, established from the intensities of the Ce and La lines, corresponds to an approximately five-fold increase in the La_2O_3 concentration relative to the average value for the specimen. In the surface film with a thickness of several atomic layers (1–1.5 nm), the La_2O_3 concentration is probably even greater, as a result of chemisorption. With increase in the La_2O_3 concentration, the line due to the new compound becomes stronger, and the lines with E_b = 882.3 eV and 882.6 eV become weaker. These data indicate that the introduction of La_2O_3 into CeO_2 leads to the formation on the surface of the CeO_2 granules of a micro-phase in which the states of the Ce atoms differ significantly from their states in CeO_2. According to the equilibrium diagram of the $CeO_2-La_2O_3$ system,[28] CeO_2 and La_2O_3 form restricted solid solutions. No chemical compounds are formed in this system. Thus in the $CeO_2-La_2O_3$ system, the chemistry of the surface micro-phases differs from the chemistry of the macro-phases. The compound formed was not identified.

Table 1 shows that, on the defects, microstructures are formed as chemical compounds which have been identified in the equilibrium diagrams ($MgAl_2O_4$, $CaTiO_3$, etc.)[9] or as compounds which are unstable in macro-volumes, for example $La_2(Cr^{VI}O_4)_3$.[9,20] In the systems with restricted solid solutions $SnO_2-Nb_2O_5$, SnO_2-NiO, SnO_2-ZnO,[9,16] and SnO_2-TiO_2, the micro-phases and the macro-phases differ in the concentration of the dissolved component.[9,15] The microstructures may be produced on the surface, and also along the boundaries of crystals and blocks and on dislocations, that is in the zones in which defects are concentrated. The crystallographic properties of the main oxide and the impurity play an important role in the formation of microstructures. The distribution coefficients of the impurities vary over a wide range, and depend on the concentration of the impurity, the nature of the interaction between the impurity and the defects of the matrix, and on temperature.

X-Ray electron spectroscopy has been used[12] to study a specimen of aluminium oxide containing 0.06 mole % MgO and 0.002 mole % CaO. The concentrations of the impurities determined along the grain boundaries were 0.2 mole % MgO and 3.4 mole % CaO, corresponding to enrichment coefficients $K = [MgO]_{boundary}/[MgO]_{bulk}$ = 3.3 and $K = [CaO]_{boundary}/[CaO]_{bulk}$ = 1700. Magnesium oxide forms surface microstructures consisting of non-stoichiometric spinel in the form of isolated units, whereas calcium oxide is distributed uniformly along the boundaries and is concentrated in several atomic layers of the surface of the crystals. A decrease in the segregation of calcium oxide is observed with increase in temperature.

In titanium oxide specimens containing added barium oxide,[9] the surface layer with a thickness of 8–10 nm was enriched in barium oxide; with increase in the concentration of the additive in the specimen, although its concentration in the surface layer increased, the distribution coefficient K decreased. In the surface layers, BaO was present as local formations with the composition $BaTiO_3$.

In the SnO_2-CaO system, the compounds $CaSnO_3$ and Ca_2SnO_4 are formed.[29] Quantitative X-ray electron analysis of the surface showed that the coefficient of enrichment of the surface layer of the specimens in calcium oxide reached 520 at a CaO additive concentration of 0.01 mole %, and 7.8 at a CaO concentration of 10 mole %.[30] In the surface layer, the tin is present as tin(IV) in an octahedral environment of oxygen atoms [SnO_6; $E_b(Sn3d_{5/2})$ = 486.7 eV], as in SnO_2. The Ca atoms have cubo-octahedral coordination, similar to that observed in $CaSnO_3$. For $CaSnO_3$ and $CaTiO_3$, $E_b(Ca2p_{3/2})$ = 347.2 eV; for CaO with calcium in octahedral coordination, the value is 346.3 eV. The $Ca2p_{3/2}$ spectrum of the compound Ca_2SnO_4, which contains calcium ions in two non-equivalent positions, is the superposition of the spectra of $CaTiO_3$ and CaO. Thus the coordination of the Ca atoms changes from octahedral in CaO to cubo-octahedral in $CaSnO_3$. Moreover, XPES data obtained with a positive charge on the surface showed that the specimens with a low CaO concentration contain two phases in the surface layer—SnO_2 (continuous layer) and $CaSnO_3$ (local formations).

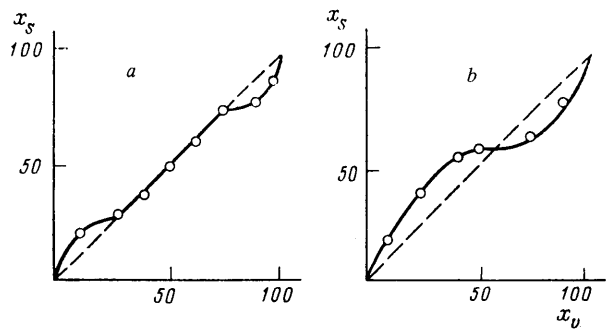


Figure 2. Composition of the surface layer of specimens in the SnO_2-TiO_2 system at different heating temperatures: *a*) 1373 K, *b*) 1673 K; x_v and x_s are the volume and surface concentrations of TiO_2.[15]

The SnO_2-TiO_2 system[15] is characterised by much smaller surface enrichment coefficients than the SnO_2-CaO system. At a concentration of 0.1 mole % TiO_2 in tin(IV) oxide, the enrichment coefficient is 11, and with the addition of 0.1 mole % SnO_2 to the TiO_2 matrix the coefficient is 50. Fig.2 gives the dependence of the composition of the surface of the specimen on its bulk composition in the SnO_2-TiO_2 system. At a heating temperature of 1373 K in the range of bulk compositions 25–75 mole % TiO_2, the surface layer is two-phase, and its composition corresponds exactly to that of the macro-volume. In the regions adjoining the pure components of the system, the surface layer is single-phase, and its composition differs from that of the bulk. Increase in the heating temperature to 1673 K leads to the formation, throughout the entire composition range, of a single-phase surface layer, whose composition differs from that of the bulk. Thus in this system, surface solid solutions TiO_2-SnO_2 are formed, and the range of their existence is broader than that for the bulk phases.

The distribution of added SiO_2 in polycrystalline SnO_2 is characterised by the following parameters.[15] With change in the quantity of added SiO_2 from 0.1 mole % to 5.0 mole %, the enrichment coefficient changes from 320 to 12. The coordination numbers of tin and silicon remain unchanged. The surface layer of the specimens is two-phase throughout the composition range.

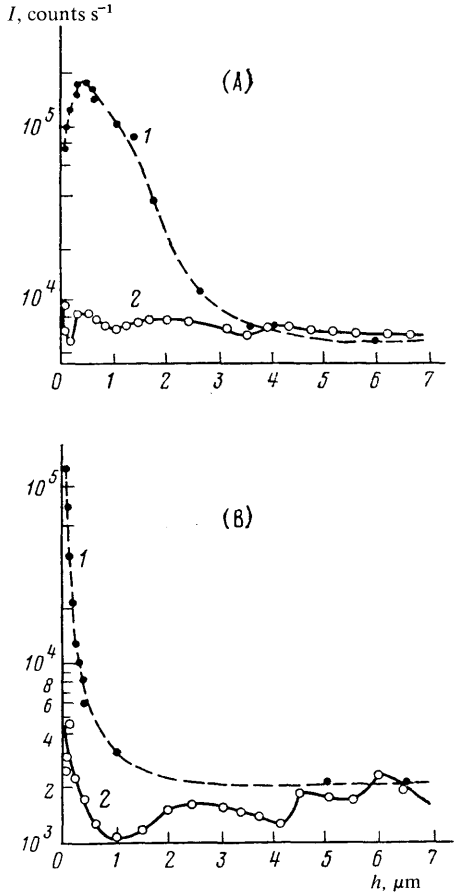


Figure 3. Mass-spectrometric microanalysis of the distribution of Al in slowly cooled (*1*) and quenched (*2*) MgO specimens containing 0.187 mass % Al (*A*) and 0.006 mass % Al (*B*); *h* is the depth of the layer analysed, *I* is the number of counts in 1 s, ^{27}Al.[11]

If the impurity forms continuous solid solutions with the oxide matrix (isomorphous systems), the internal adsorption of the isomorphous impurity is slight, $K \simeq 1$. The compounds NiO and MgO form a continuous series of solid solutions.[29] An XPES analysis of polycrystalline magnesium containing NiO showed that the concentration of nickel oxide in the surface layer is practically the same as that in the bulk.[9] The Ni2$p_{3/2}$ and Mg2$s_{1/2}$ binding energies in the surface layer of the specimen are the same as in the pure oxides. This indicates that solid solutions of NiO in MgO are formed both in the surface layer and in the bulk.

The stability and concentration of the microstructures on the defects change with change in temperature. The dependence of the surface segregation of Al_2O_3 in MgO on the thermal treatment conditions has been studied.[11] Single crystals of magnesium oxide containing 0.187 mass % and 0.006 mass % Al in solid solution [specimens (A) and (B) respectively] were heated in air for several hours at a temperature of 2073 K. Half of the specimens were subjected to air quenching by ejection from the furnace, and the rest were cooled in the furnace over a period of several hours. The results of the experiments are given in Fig.3. In the specimen cooled slowly (A), the maximum concentration of Al was established at a depth of less than 1 μm from the surface. Microscope and mass-spectrometric analyses showed the formation of local inclusions of spinel in the surface layers. The quenched specimen showed little change in the concentration of aluminium in the layer next to the surface, and no heterogeneous formations were detected. At high temperatures, desorption and solution of Al_2O_3 in the bulk of the MgO crystal take place. On slow cooling, segregation of Al_2O_3 developed on the defects, and the formation of microstructures with the composition $MgAl_2O_4$ was observed. Similar processes took place in the (B) specimens. Comparison of the curves for specimens (A) and (B) shows that the depth of formation of the microstructures increases with increase in the concentration of impurity.

The kinetics of the segregation of Al_2O_3 on the defects in an MgO matrix have been studied.[31] The rate of separation of Al_2O_3 from the $MgO-Al_2O_3$ solid solution and the formation of spinel along the grain boundaries increase with increase in the concentration of the dissolved component. The process is controlled by diffusion.

Table 2. Primary products of the chemical reaction in oxide mixtures.

Systems	Primary products	*A*	Refs.
$MgO-Al_2O_3$	$MgAl_2O_4$	1:1, 1:13	[34]
$CaO-Al_2O_3$	$CaAl_2O_4$	3:1, 12:7, 1:1, 1:2, 1:6	[34]
$SrO-Al_2O_3$	$SrAl_2O_4$	3:1, 2:1, 1:1, 1:2, 1:6	[34]
$BaO-Al_2O_3$	$BaAl_2O_4$	3:1, 2:1, 1:1, 1:6	[34]
$CaO-Fe_2O_3$	$Ca_2Fe_2O_5$	2:1, 1:1, 1:2	[34]
$MgO-SiO_2$	Mg_2SiO_4	2:1, 1:1	[34]
$CaO-SiO_2$	Ca_2SiO_4	3:1, 2:1, 3:2, 1:1	[34]
$CrO-SiO_2$	Sr_2SiO_4	2:1, 1:1	[34]
$BaO-SiO_2$	Ba_2SiO_4	2:1, 1:1, 2:3	[34]
$MgO-TiO_2$	$MgTiO_3$	2:1, 1:1, 1:2	[34]
$CaO-TiO_2$	$CaTiO_3$	3:1, 2:1, 1:1	[34]
$BaO-TiO_2$	$BaTiO_3$	1:1, 1:2, 1:3, 1:4	[34]
$PbO-MoO_3$	$PbMoO_4$	2:1, 1:1	[34]
$PbO-WO_3$	$PbWO_4$	2:1, 1:1	[34]
$Y_2O_3-Al_2O_3$	$Y_4Al_2O_9$, $YAlO_3$	2:1, 1:1, 3:5	[22, 35, 37]
$Y_2O_3-Fe_2O_3$	$YFeO_3$	1:1, 3:5	[22]
$*Ln_2O_3-Fe_2O_3$	$LnFeO_3$	1:1, 3:5	[22]
$Ln_2O_3-Al_2O_3$	$LnAlO_3$	1:1, 1:11	[13]
$CaO-SnO_2$	$CaSnO_3$	2:1, 1:1	[14, 34]
$CaO-ZrO_2$	$CaZrO_3$, $CaZr_4O_9$	1:1, 1:4**	[17, 18]
$La_2O_3-Cr_2O_3$	$La_2(CrO_4)_3$	1:1	[21, 22]

Note. *A* is the molar ratio of the oxides in the final products.

*Ln = La, Ce, Pr, Nd.

**Solid solution based on ZrO_2.

An X-ray electron study[9,14] of polycrystalline tin(IV) oxide containing small quantities of added calcium oxide showed that the surface layer with a thickness of 8–10 nm is enriched in calcium oxide; the enrichment coefficient *K* reached values of 520 and 7.8 for concentrations of the additive of 0.01 mole % and 10 mole %

respectively. The surface was two-phase; the SnO_2 matrix contained local formations of $CaSnO_3$. The formation of the surface layer and its stability at high temperatures were studied. The surface layer was removed by grinding. The specimens were heated to different temperatures, kept for 1 h, and then subjected to air quenching to preserve the distribution of the additive, established at the given temperature. After each thermal treatment, the spectra of the surface of the specimen were recorded, and their intensities were used to calculate the Ca/Sn ratio. At low heating temperatures with treatment for 1 h, the surface structure did not form at all. The maximum segregation (Ca/Sn = 0.53) wa attained at 1773 K. At higher temperatures, the reverse process, that is the solution of the microstructure in the matrix, took place.

The depth (thickness) of the surface formations in crystalline oxides varies over a wide range and depends on the nature and concentration of the impurities present in the surface structures. Fig.3 shows that the boundaries of the surface formations, facing into the crystals, have an indistinct "diffuse" form. With increase in the concentration of impurity, the depth of segregation increases. The depth of segregation of the impurities at the grain boundaries also depends on temperature, and increases with increase in the latter.[32]

The surface and the grain boundaries of oxides have an electric charge, as a consequence of the presence of an excess of ions of a given sign.[32] This surface charge is compensated by ions of opposite sign, which are formed close to the surface and extend to a depth of 2–10 nm.

IV. THE RELATIONSHIP BETWEEN THE CHANGE IN THE DEFECT CHARACTER AND THE SEQUENCE OF CHEMICAL REACTIONS IN MIXTURES OF SOLID OXIDES

Solid-phase reactions generally take place in several stages. Irrespective of the reagent ratio in the original mixture, the intermediate reaction product is a definite compound.[13,17,22,34–37] Examples of these reactions are given in Table 2.

It has been suggested[34] that the compound with the highest crystallisation temperature is formed first. This rule is not confirmed by a number of reactions, however. For example, in mCaO + $n$$Al_2O_2$, mMgO + $n$$TiO_2$, and $m$$Y_2O_3$ + $n$$Al_2O_3$ mixtures, irrespective of the component ratio, the compounds $CaAl_2O_4$, $MgTiO_3$, and $YAlO_3$ respectively are formed in the first stage of the reaction. According to the equilibrium diagrams of the $CaO-Al_2O_3$, $MgO-TiO_2$, and $Y_2O_3-Al_2O_3$ systems,[29] the compounds formed first are not the most refractory. The physicochemical factors causing solid-phase reactions to take place in stages have been studied.[20]

Comparison of the formation of microstructures in oxides containing impurities (Table 1) and the primary reaction products of the corresponding oxides in solid-phase reactions (Table 2) shows that defects play a definite role in these processes. In reacting oxide mixtures, the compounds formed first are those which are also produced on defects in the oxides.[20] For example, in mMgO + $n$$Al_2O_3$, mCaO + $n$$SnO_2$, mCaO + $n$$TiO_2$, and mBaO + $n$$TiO_2$ mixtures, irrespective of the component ratio, the compounds $MgAl_2O_4$, $CaSnO_3$, $CaTiO_3$, and $BaTiO_3$ respectively are formed first. On the other hand, in the same systems, but at concentrations of the second components from 0.01 mole % to 1 mole % (see Table 1), the compounds $MgAl_2O_4$, $CaSnO_3$, $CaTiO_3$, and $BaTiO_3$ respectively are formed as local microstructures on defects.

In a 2CaO + SnO_2 mixture at temperatures of 1200–1500 K, reactions take place to give the primary product $CaSnO_3$, and when the reaction mixture contains sufficient calcium oxide, this product reacts further with it to give the compound Ca_2SnO_4.[34]

Solid-phase chemical reactions are accompanied by a change in the defect character of the reacting mixture. According to Ref.34, the chemical reaction involves a number of elementary processes: covering of the surface, breakdown of the crystals and disordering as a result of surface and bulk diffusion, actual chemical reaction, an increase in the specific surface of the reacting substances, subsequent formation of a defect crystalline product, and removal of the defects in the crystal lattice of the compound formed. At definite stages, these processes lead to an increase and then a decrease in the defect character of the reacting mixture.

In the synthesis of compounds with the garnet structure $A_3B_5O_{12}$, where A = Ln, Y, and B = Al, Fe, the solid-phase reactions in the $3A_2O_3$ + $5B_2O_3$ mixtures take place with the formation of monoclinic $Y_4Al_2O_9$ and cubic $YAlO_3$ as intermediate products.[22,36] For this reason, it is difficult to obtain the pure product $A_3B_5O_{12}$.

An X-ray electron spectroscopic study[20] of the synthesised compound $Y_3Al_5O_{12}$ in the surface layer of a specimen with a thickness of 7–10 nm established the ratio Y/Al = 1.03 ± 0.05, which corresponds to the compound $YAlO_3$. The $Al2s_{1/2}$ binding energy in the surface layer is 119.2 ± 0.1 eV. In the compounds $YAlO_3$ and $LaAlO_3$, aluminium is in octahedral coordination, $E_b(Al2s_{1/2})$ = 119.3 ± 0.1 eV. For aluminium in tetrahedral coordination in sodalite $3NaAlSiO_4.NaCl$, E_b = 118.2 ± 0.1 eV. In the garnet structure, Al occupies tetrahedral positions. On the surface of the specimen with the composition $Y_3Al_5O_{12}$, aluminium was detected in octahedral coordination. The composition of the surface and the octahedral coordination of aluminium indicate that microstructures of the compound $YAlO_3$ are formed in the defect surface layer of the specimen with the composition $Y_3Al_5O_{12}$. $YAlO_3$ microstructures may also be produced along the boundaries of the crystals and blocks and on dislocations, that is in the zones where defects are concentrated. Thus in the $3Y_2O_3$ + $5Al_2O_3$ reaction mixture, the intermediate compounds $YAlO_3$ and $Y_4Al_2O_9$ are formed in the initial period of intensive defect formation.

In the systems given in Table 2, the intermediate reaction products of the oxides are generally found on the corresponding equilibrium diagrams. The formation on defects of new microstructures with compositions and structures differing from those of the equilibrium compounds is also possible, however. An example is provided by the $Cr_2O_3-La_2O_3$ system.

In an La_2O_3 + Cr_2O_3 mixture at a temperature of 873 K, phases corresponding to the chromate $La_2(CrO_4)_3$ and the chromite $LaCrO_3$ were detected in addition to the original oxides[20,22] (Fig.4). The kinetic curve *3* (the formation of the intermediate chromate) has a maximum indicating the predominant formation of chromate in the initial stage of the reaction of chromium(VI) according to the scheme

$$1.5Cr_2O_3+2.25O_2+La_2O_3\rightarrow La_2(CrO_4)_3.$$

The course of curve *3* is determined by two factors: the change in the defect character of the reaction mixture, which is responsible for the production of the maximum, and the presence of lanthanum oxide, which binds Cr^{VI} in a chemical compound.[20]

XPES has established the formation of metastable microstructures $xCr_2O_3.yCrO_3$ on defects in a Cr_2O_3 matrix,[38] the concentration of which decreases with increase in temperature and with decrease in

the oxygen pressure in the gaseous medium.[21] Metastable microstructures influence the reactivity and catalytic activity of substances, and the sintering and recrystallisation of solids.[10,16,20,21,39]

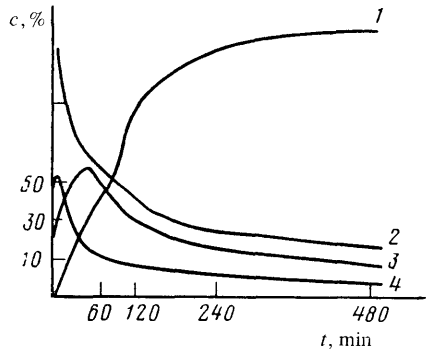


Figure 4. Kinetics of the reactions in an $La_2O_3 + Cr_2O_3$ mixture in air at 873 K; *c* is the concentration: *1*) $LaCrO_3$, *2*) La_2O_3, *3*) $La_2.(CrO_4)_3$, *4*) Cr_2O_3.[20,22]

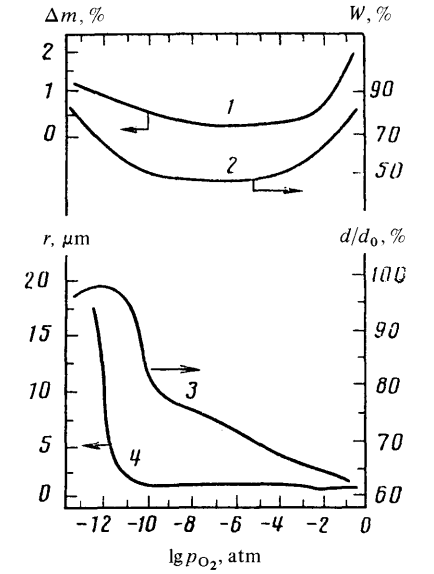


Figure 5. Change in the volatility, reactivity, sintering, and collective recrystallisation of chromium oxide on the partial pressure of oxygen:[21] *1*) mass loss (Δm) after 1 h at 1870 K;[40] *2*) quantity (W) of bound chromium oxide formed by the reaction $MgO + Cr_2O_3 = MgCr_2O_4$ after 1 h at 1620 K;[21] *3*) relative density (d/d_0) of chromium oxide specimens, sintering at 1870 K, 1 h;[40,41] *4*) size of the crystals (r), heating at 1970 K for 1 h.[21]

The results of studies[21,40–42] of the dependnece of the properties of chromium oxide and its compounds on the partial pressure of oxygen are given in Fig.5. The most intensive mass loss by a specimen of chromium oxide at a temperature of 1873 K (curve *1* in Fig.5) takes place at an oxygen pressure of 1 atm. This high volatility is due to the following features. At increased temperatures, chemical adsorption of oxygen on Cr_2O_3 crystals takes place,[21,43] to give oxygen-containing surface compounds of chromium with an increased valence $CrO_{1.5+x}$ (CrO_3, CrO_2), which are highly volatile. With decrease in the partial pressure of oxygen, the volatility of the specimens decreases. In the oxygen pressure range $10^{-3}-10^{-5}$ atm, the surface compounds $CrO_{1.5+x}$ become unstable, and their concentration decreases, and with further decrease in p_{O_2} they may may not be formed.

At low partial pressures of oxygen ($10^{-10}-10^{-13}$ atm), the volatility of the specimens increases again. Under these conditions, chromium oxide dissociates on the surface of the particles according to the scheme

$$^2/_3Cr_2O_3 \rightleftarrows {}^4/_3Cr + O_2 .$$

The rate of the reaction $MgO + Cr_2O_3 \rightarrow MgCr_2O_4$ (curve *2*) and the volatility of chromium oxide (curve *1*) change in the same sense with change in the partial pressure of oxygen. The activating factors in these processes are, firstly, the formation of the surface compounds $CrO_{1.5+x}$ at a high oxygen pressure of $10^{-2}-1$ atm, and, secondly, the predissociation of Cr_2O_3 at a low oxygen pressure of $10^{-10}-10^{-13}$ atm.

The rates of the sintering (curve *3*) and collective recrystallisation (curve *4*) of chromium oxide in oxygen (1 atm) and in air are reduced considerably. After heating at temperatures of 1870–2020 K for 1 h in the gaseous media indicated, the specimens remain porous and finely crystalline. Intensive sintering and crystal growth begin at oxygen pressures of $10^{-10}-10^{-11}$ atm and $10^{-11}-10^{-12}$ atm respectively. This effect of the surface compound $CrO_{1.5+x}$ is determined by the thermodynamic conditions on the surface of the particles. The formation of $MgCr_2O_4$ from the oxides at 1273 K takes place with $\Delta H = -10.3$ kcal and $\Delta G = -8.1$ kcal mole^{-1}.[21] The heats of sintering of the oxides are apparently comparable with the heats of the change from the amorphous to the crystalline state (1–3 kcal mole^{-1} [21]). The heats of collective recrystallisation are probably of the same order of magnitude as the energies of polymorphic transformations (0.01–1 kcal mole^{-1} [21]). The heat of adsorption of oxygen on the surface of chromium oxide, calculated from the equilibrium isobar, is 3.7 kcal mole^{-1}.[21]

The suppression of the sintering and recrystallisation of chromium oxide by adsorbed oxygen (p = 1 atm) is possible if ΔG_0, that is the thermodynamic potential of the formation of the surface compound $CrO_{1.5+x}$, is greater than the thermodynamic potential of the sintering or collective recrystallisation (ΔG_s) of chromium oxide: $\Delta G_a > \Delta G_s$, where ΔG_a relates to the adsorption of oxygen (here, the absolute values of the thermodynamic potentials are understood). The thermodynamically more stable surface compound prevents the decrease in the surface which takes place on sintering and collective recrystallisation. If the partial pressure of oxygen is lowered to values at which $\Delta G_a < \Delta G_s$, intensive sintering and recrystallisation of chromium oxide begin, as observed experimentally. The activation of the formation of chromium spinel at p_{O_2} = 1 atm is due to the fact that $\Delta G_0 > \Delta G_a$. The higher activity of the surface compound $CrO_{1.5+x}$ is due to the fact that its dissociation pressure is higher than that of Cr_2O_3. The dissociative activation of the surface compound reaches a maximum value at thermodynamic equilibrium, that is on fulfilment of the condition $\Delta G = RT \ln(p_{O_2}/p^*) = 0$, where p^* is the dissociation pressure of the surface compound $CrO_{1.5+x}$.

In the high-temperature synthesis of oxide materials, the water vapour which is always present in the furnace atmosphere is adsorbed on the oxide particles and activates the physicochemical processes taking place. A study[4] of the influence of the presence of oxygen and water vapour on the kinetics of the reactions of the oxides MgO, CaO, BaO, and ZnO with Al_2O_3 and of CaO with quartz and amorphous silica showed that at increased temperatures in an oxygen atmosphere and more particularly in the presence of water vapour the oxides are more reactive than in a vacuum. The surface complexes formed, MO_{n+x} or $MO_n.xH_2O$, activate crystallisation and sintering and increase the reactivity of the material.[44]

V. THE MECHANISM OF THE ACTION OF IMPURITIES IN SINTERING, AND THE DEFORMATIONAL PROPERTIES AND THERMAL STABILITY OF OXIDE MATERIALS

The mechanism of the activating and inhibiting action of impurities on physicochemical processes in solids is not completely clear, and a single theory has not been developed. The most widely accepted model is that in which disorder is produced in the lattice of the matrix by ions with a different valence as a result of a change in the concentration of vacancies in the anion or cation sublattices. Many experimental data are difficult to explain using this model, however.

As shown in sections III and IV of the present review, impurities react with defects of the matrix and in micro-volumes to form compounds differing in their composition, structure, and energy from the defect-free regions of the matrix. Thus real solids are microheterogeneous systems. To investigate the mechanisms of the processes taking place in these systems, it is necessary to study the chemical composition, structure, and energy state of the formations in local micro-volumes.

The effect of added Ln_2O_3 (Ln = lanthanide) on the kinetics of the sintering of cerium oxide has been studied.[10,13,45] According to the equilibrium diagrams,[13,29] these oxides in the concentration range 0–10 mole % Ln_2O_3 studied react with cerium oxide to form solid solutions with the fluorite structure. The results of experiments to study the influence of added lanthanum oxide on the shrinkage of cerium oxide are given in Fig.6. The Ln_2O_3 impurity forms a chemical compound on the defects of the CeO_2 matrix (see Table 1). The formation of the microstructure should pass through a stage involving the formation of a eutectic, depending on the concentration of the additive.

In the primary sintering of mechanical mixtures of the powders (curve *1* in Fig.6), when the additives have not yet penetrated into the cerium oxide particles, the effective concentration of the additive on the surface of the cerium oxide particles is much greater than that corresponding to its final (equilibrium) distribution (curves *2* and *3* in Fig.6), and the critical state of the microstructures is produced at a lower actual concentration of the additive (0.5 mole % Ln_2O_3). On the second and third heating of the specimens (curves *2* and *3* in Fig.6), the maximum intensities of sintering correspond to an additive concentration of 1.25 mole % Ln_2O_3. With further increase in the additive concentration of 1.25 mole % Ln_2O_3. With further increase in the additive concentration (> 1.25 mole %), a decrease in the rate of sintering is observed, and the additive acts as an inhibitor (range of the stable state of the microstructures). With increase in the sintering temperature to 1873 K, the shrinkage maximum becomes flatter, and at 1923 K the additive activates the sintering throughout the concentration range studied. As shown in section III, the stability and concentration of the microstructures changes with change in temperature. At 1923 K, the microstructures "dissolve" in the CeO_2 matrix.

The results of experiments[45] to study the influence of single (Sm_2O_3) and combined (Sm_2O_3 + Gd_2O_3) and (Sm_2O_3 + Gd_2O_3 + Y_2O_3) additives on the sintering of cerium oxide show that the effect of the added mixtures is additive, since the valences are the same, and the structures of the electron levels and the ion dimensions are similar: $R(Sm^{3+})$ = 0.97 Å, $R(Gd^{3+})$ = 0.94 Å, $R(Y^{3+})$ = 0.97 Å.[45] In the mixtures containing (98 – *x*) mole % CeO_2 + 2 mole % La_2O_3 + *x* mole % Sm_2O_3, increase in the samarium oxide concentration is accompanied by a regular decrease in the shrinkage of the cerium oxide specimens. The reason for this behaviour of the mixtures is that lanthanum oxide forms more stable microstructures than samarium oxide. The change in the shrinkage when the complex additives La_2O_3 + Y_2O_3(Sm_2O_3) are used[45] is similar to that when only lanthanum oxide is added. Preferential internal adsorption of lanthanum oxide apparently takes place as a result of the higher energy of interaction with the defects of the matrix for lanthanum ions compared with yttrium or samarium ions.

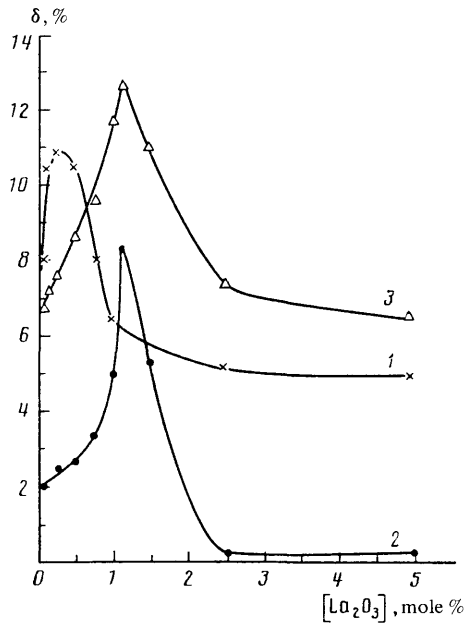


Figure 6. Dependence of the linear shrinkage (δ, %) of cerium dioxide on the concentration of added La_2O_3: *1*) first sintering (1673 K, 0.5 h); *2*) second sintering (1673 K, 2 h); *3*) third sintering (1773 K, 2 h).[10,45]

The results of experiments on the sintering of mixtures with the composition (80 – *x*) mole % CeO_2 + 20 mole % Nd_2O_3 + *x* mole % La_2O_3 in which *x* varied from 0 to 5 show that at the concentration indicated, the additives have an inhibiting action on the sintering of cerium oxide. A maximum was not observed, and the system showed only a regular poorly defined decrease in the rate of shrinkage, indicating that the effect of the reagents is additive. These experiments indicate that the added oxides M_2O_3 (from La to Yb, and also Y) react with the same defects of the CeO_2 matrix.

The properties of a modified cerium oxide ceramic have been studied.[39,47,48] In the range of additive concentrations 0.5 to 1.25 mole % La_2O_3, an extremal change in properties was observed. The processes of sintering, deformation, and crystal growth took place at maximum rates. The ceramic with the composition indicated had the optimum catalytic activity in the dehydrogenation of isopropyl alcohol.[49] With both decrease and increase in the additive concentration, the rate of sintering, deformation, and catalytic activity decreased, with corresponding changes in other properties.

Analysis of the results indicates a single mechanism of action of the microstructures on the processes being considered. The highest activity is observed when the thermodynamic state of the microstructure corresponds to the critical state where $a^0 = a_m$, $\Delta G_d = RT \ln(a^0/a_m) = 0$, where ΔG_d is the change in free energy on dissociation of the microstructure, a^0 and a_m the activity of the additive in the bulk of the crystal and in the microstructure respectively, R the gas constant, and T the temperature.

When the concentration of the impurity in the solid is lower than the equilibrium concentration and $a_m > a^0$, $\Delta G_d = RT \ln(a^0/a_m) < 0$, the microstructure is not formed, so that the additive does not have an activating effect.

The rate of deformation of the cerium ceramic is determined by the concentration of La_2O_3 in it. The efficiency of the influence of the microstructures formed by the impurities also depends on the temperature of the thermomechanical testing.[47,48]

With increase in the temperature of testing from 1473 K to 1573 K, the rate of deformation changes in different ways for specimens with different compositions. The fluidity increases considerably in the specimens containing 1.25 mole % La_2O_3, and is practically unchanged in the ceramic containing 5 mole % La_2O_3. With increase in temperature, the intensity of the relaxation processes evidently increases to the greatest extent in the thermodynamically unstable microstructures.

The increased thermal stability of the specimens containing 0.5 to 1.25 mole % La_2O_3 can be attributed to the high rate of the relaxation processes in the microstructures. According to phenomenological theory,[48,50] the stability of a material to thermal shock is due to the interaction of three forms of energy: the energy of elastic deformation, the surface energy, and the kinetic energy associated with the formation and growth of cracks. Expressions giving the relationship between the surface energy and the thermal stability of a material are given below. The Griffiths stress σ_g required to create cracks with dimensions c is related to the surface energy by the equation $\sigma_g^2 = 2\gamma E/\pi c$, where γ is the surface energy of the material, and E the modulus of normal elasticity.[48,50] The maximum temperature differential for which growth of cracks does not take place is given by

$$\Delta T = \left(\frac{2\gamma}{\pi c E}\right)^{1/2} \frac{1 + 2Nc^2}{\alpha}$$

where N is the number of cracks in the material on unit area, and α the coefficient of thermal expansion. In Ref.50 it is recommended that a material with a high surface energy be selected for articles subjected to thermal shock during use.

In the region of the critical state ($\Delta G_d = 0$), substances of different character show a heat capacity maximum;[51] as a result, the substances acquire an excess of energy by absorbing heat from the surrounding medium.

Under the conditions being considered, the surface structures in specimens of a CeO_2 ceramic containing 0.5 – 1.25 mole % La_2O_3 apparently have an excess of energy compared with the microstructures in specimens with either higher or lower La_2O_3 concentrations.

The catalytic action of the additives is due to the fact that the surface complexes in the critical state, formed as a result of the reaction of the substrate with the catalyst, have the highest reactivity and act as active centres in the transformation of the substrate.[39]

The microstructures forming restricted solid solutions on defects, and their influence on the thermomechanical properties of oxide ceramic materials, are examined below. In the $TiO_2 - Ta_2O_5$ system, XPES established[10] that in a surface layer with a thickness of 8 – 10 nm, tantalum is present as tantalum(V) in an octahedral environment of oxygen ions, as in Ta_2O_5.

Increase in the additive concentration is accompanied by an increase in the concentration of Ta_2O_5 in the surface layer, but its distribution coefficient decreases.[10]

[Ta_2O_5], mole %, in the bulk	0.001	0.1	3.0	5.0	10.0
[Ta_2O_5], mole %, in the surface layer	0.02	0.5	8.0	10.0	15.0
Distribution coefficient (K)	20	5	2.6	2	1.5

Experimental data[25] indicate that Ta_2O_5 dissolves in titanium oxide as the rutile-like compound $Ti^{III}TaO_4$. The possible formation of a solid solution in the $TiO_2 - Ti^{III}TaO_4$ system when titanium dioxide is added is due to the reduction of rutile in air at a temperature above 1370 K and the stabilisation of Ti^{III} when introduced into the solid solution.

At low concentrations (1 – 4 mole % Ta_2O_5), the additive had an inhibiting action on the sintering, and also lowered the fluidity and thermal stability of the ceramic at high temperatures. At a higher concentration of the additive, the rate of sintering, deformation, and thermal stability of the specimens increased. The dependence of the properties of the TiO_2 ceramic on the Ta_2O_5 concentration is given by curves with minima, correlating with the corresponding relationship for the free energy of the restricted solid solution.[46]

Similar relationships were established[16] in a study of the sintering of SnO_2 containing added Nb_2O_5. Increase in the concentration of added Nb_2O_5 from 0 to 0.05 mole % leads to suppression of the sintering; the shrinkage decreases from 11% to 6.3%. With further increase in the Nb_2O_5 concentration, intensification of the sintering is observed. Analysis of the X-ray electron spectra of specimens with the composition 99.8 mole % SnO_2 + 0.2 mole % Nb_2O_5 and 98 mole % SnO_2 + 2 mole % Nb_2O_5 showed enrichment of the surface layer in niobium by factors of 27 and 7 respectively. The energy parameters and valences of the Sn^{4+} and Nb^{5+} ions in the surface layer were the same as in SnO_2 and Nb_2O_5. In the surface layer of the tin(IV) oxide specimen, the added Nb_2O_5 forms restricted solid solutions, which are supersaturated at a concentration of 0.5 mole % or more Nb_2O_5. The solubility of Nb_2O_5 in SnO_2 is ~3 mass %.[52] Similar surface microformations were found in the $SnO_2 - ZnO$ system.[16] The surface phase consists of a solid solution with restricted solubility, with a higher concentration of the dissolved component, compared with the solid solution in the bulk.

Studies of various properties of an SnO_2 ceramic containing added ZnO showed that at concentrations of 0 – 0.5 mole % ZnO the shrinkage and thermal stability of the specimens remained unchanged, but the rate of sublimation decreased, corresponding to the existence of stable solid solutions in the surface layers. At ZnO concentrations greater than 0.5 mole %, its activating influence increased as a consequence of the decomposition of the surface solid solutions.

One promising method for preparing oxide materials with specified properties is by using modifying agents. Depending on their thermodynamic state, the microstructures formed by the impurities

may have either an activating or an inhibiting action on the physicochemical processes in the oxides in the synthesis and application of ceramic materials. If the impurity forms a chemical compound on the defects in the matrix, the formation of the micro-structure should take place via the stage of eutectic formation, depending on the concentration of the additive. Thermodynamic analysis[46] shows that the eutectic has the highest free energy, and the micro-formations in the eutectic state have the maximum reactivity. The critical state of the microstructure is reached at a definite concentration of the additive.

When the impurity forms solid solutions on the defects, activation is achieved in the critical state of the system, corresponding to supersaturation of the restricted solid solutions.

The established regularities of the formation of microstructures make it possible to use micro-additives to control the sintering and recrystallisation of dispersed solids, and also to produce specified properties such as the deformation, thermal stability, and ageing of ceramic materials at high temperatures.[9,10,16,39]

VI. SURFACE MICROSTRUCTURES AND THE PROTECTION OF CERAMIC MATERIALS FROM REDUCTION

One of the most important tasks in materials science is the production of ceramic condenser materials permitting high-temperature annealing in media with a low partial pressure of oxygen without loss of the dielectric properties. This task follows directly from the problem of replacing electrodes of valuable metals in ceramic condensers by electrodes of non-noble metals, whose annealing can be carried out only in a protective atmosphere with a low partial pressures of oxygen.

The processes taking place in the synthesis of materials permitting annealing in gaseous media with a low oxygen pressure have been described using the theory of point defects and the method of quasi-chemical reactions.[53–55] In the works cited, the equilibrium state of the point defects is assumed *a priori*, and the influence of impurities and additives on the properties of the material is regarded as a displacement of the equilibrium according to the law of mass action applied to the point defects. This model does not take account of physicochemical processes and the formation of surface microstructures.

XPES data[24,56] show that when additives which protect calcium titanate from reduction are introduced, the surface of $CaTiO_3$ granules has the composition $3CaO.TiO_2$, that is it differs from calcium metatitanate. The increase in the stability of the $CaTiO_3$ ceramic to reduction must be related to the formation of a surface structure which is enriched in CaO and which has an equilibrium oxygen pressure lower than that in the moist hydrogen used for annealing the ceramic. So long as reduction does not affect the surface phase, reduction of $CaTiO_3$ in the bulk does not take place, but the non-doped material may be reduced to a considerable extent under these conditions. The reduction begins at the surface, that is the defect zone, which moves into the depth during the process. The surface structure $3CaO.TiO_2$ formed increases the thermodynamic stability of the surface and the grain boundaries. Increase in the temperature of annealing and decrease in the partial pressure of oxygen in the furnace lead on prolonged treatment to reduction of the surface structure and the material in the bulk.

Similar results were obtained in a study of the protection of $SrTiO_3$ from reduction by adding SrO, BaO, MgO, and Ga_2O_3.[57] According to XPES data, in the specimens containing added Ga_2O_3, after heating in moist hydrogen, the surface layers of the ceramic did not contain gallium, because of the reduction of Ga_2O_3 to Ga_2O, which volatilised. Thus in the specimens in which titanium was replaced by gallium, the surface of the strontium titanate granules was enriched to the composition $\sim 7SrO.TiO_2$.

Examination of the reduction process from the viewpoint of surface phase formation makes it possible not only to obtain a consistent explanation of available experimental data but also to make specific technological recommendations for the production of materials which can be heated in media with a low partial pressure of oxygen.

VII. THE INFLUENCE OF SURFACE STRUCTURES ON THE ELECTRICAL PROPERTIES OF CERAMIC MATERIALS

Oxide materials with dielectric, semiconducting, or highly conducting properties with electronic or ionic carriers are synthesised by controlling the chemical character and concentration of impurities. The mechanism of the action of the impurities has been insufficiently studied, however.

The titanium-containing compounds TiO_2, $CaTiO_3$, $SrTiO_3$, and $BaTiO_3$ and solid solutions based on them are widely used in electronics. The properties of TiO_2 containing Ta_2O_5 have been studied.[58] In Ref.59 it was suggested that the semiconducting properties of doped titanium dioxide are due to the production of titanium(III), but the reasons for its appearance were not established. Magnetochemical and XPES data [58] showed that Ta_2O_5 dissolves in titanium dioxide to give the rutile-like compound $Ti^{III}TaO_4$. The possible formation of a solid solution when titanium dioxide is doped is due to the reduction of rutile in air at a temperature above 1370 K and the stabilisation of Ti^{III} in the solid solution.[13] The formation of the $TiO_2-Ti^{III}TaO_4$ solid solution leads to a decrease in the specific electrical resistance of the specimens by factors of 10^8-10^{10} at concentrations of 0.1–5 mole % Ta_2O_5. When the limit of the solubility of Ta_2O_5 in TiO_2 at the grain boundaries is exceeded, decomposition and oxidation of the $TiO_2-Ti^{III}TaO_4$ solid solution takes place to give dielectric layers with the composition $TiO_2 + TiTa_2O_7$ on the surface of the granules. Thus the extremal concentration dependence of the conductivity of TiO_2 doped with Ta_2O_5 is due to two competing reactions: the formation and decomposition (oxidation) of the $TiO_2-Ti^{III}TaO_4$ solid solution.[57]

The influence of the combined additives Nb_2O_5 and BaO on the electrophysical properties of TiO_2 has been studied.[60] When the niobium(V) cations are added, the specific electrical resistance of the material decreased from 10^{13} Ω.cm to 100 Ω.cm at 300 K. Auger spectroscopy detected the segregation of barium along the grain boundaries of the titanium dioxide ceramic; the distribution coefficient of barium reached 150. The action of the added Nb_2O_5 was explained[60] using the disordering model:

$$Nb_2O_5 = 2Nb_{Ti}^{\cdot} + 2e^- + 4O_O + {}^1/_2O_2$$

where $Nb_{Ti}^{\cdot}$ is the cation occupying a cation site in the TiO_2 lattice; O_O an oxygen ion in a normal position (in a lattice site); and e^- an electron. This approach is inadequate, since it does not reveal the detailed mechanism of the physicochemical processes taking place in the reaction between the impurity and the matrix.

Niobium is an analogue of tantalum, and the formation and decomposition of the $TiO_2-Ti^{III}NbO_4$ solid solutions and the redox processes $Ti^{IV} \rightleftarrows Ti^{III}$ evidently determine the electrophysical properties of doped titanium dioxide. In Refs.58 and 61–64 it was shown

that the extremal dependence of the electrophysical properties of barium titanate when it is doped with the oxides of the lanthanides and the group V elements, so-called donor additives, is due to two competing processes in the barium titanate ceramic. On the one hand, semiconducting solid solutions containing titanium(III) [for example $Ba_{1-x}Y_x(Ti^{IV}_{1-x}Ti_x)O_3$] are formed, and on the other hand, oxidation and decomposition of the solid solutions take place (for example to give the compounds $BaTiO_3$ and $Y_2Ti_2O_7$), beginning on the surface and along the grain boundaries, as a result of which surface dielectric layers are produced. These physicochemical processes determine the extremal change in the properties of doped barium titanate: the magnetic susceptibility maxiimum, the dielectric–semiconductor transitions, and the existence of a positive temperature coefficient of electrical resistance close to the Curie point.

Materials whose properties are determined by the surface phases are used in electronics. These materials are used to prepare posistors (semiconducting ceramic devices having a positive temperature coefficient of electrical resistance), varistors (devices for which the dependence of the current on the voltage is appreciably non-linear), and condensers with an inter-granular capacity, in which a superhigh effective dielectric constant is produced since the capacities are included at the boundary of each granule. A ceramic for varistors based on zinc oxide has been studied repeatedly by electron microscopy. The segregation of Bi in a $ZnO-Bi_2O_3$ ceramic has been detected[65] at the boundary between the granules of the main material. The chemical form of the additive (MnO or MnO_2, CoO or Co_2O_3) has a significant influence on the distribution of the cations at the grain boundary and in the phase between the granules, and hence on the recrystallisation and microstructure of the specimen.[66] This is undoubtedly due to the formation of different surface structures when the oxides of metals in different oxidation states are added. Thus the monoxides MnO and CoO form solid solutions with ZnO, whereas when MnO_2 and Co_2O_3 are added, the spinels Zn_2MnO_4, $ZnMn^{III}_2O_4$, and $ZnCo_2O_4$ may be formed at the ZnO grain boundaries.

In an $SrTiO_3$ ceramic containing added Bi_2O_3, enrichment of the surface regions of the granules in Bi to a depth of up to 25 nm has been detected.[67] The influence of additives forming surface structures on the melting point of the layer at the grain boundaries, which plays a decisive role in crystallisation processes, has been noted.[68] It is suggested that selective fusion takes place, when the additives dissolve (fuse) the titanium dioxide which is always present in strontium titanate ceramic, with almost no change in the volume of the granule. An analysis of a large amount of experimental material led to the conclusion[69] that in a ceramic based on $SrTiO_3$ with added glass-forming oxides (Bi_2O_3, PbO, SiO_2): a) the second phase is concentrated in "pockets" at contacts between three granules; b) in general, the structure at the intergranular boundary is the same as that in the bulk, and the foreign ions merely enrich the outer layers of the granules; and c) the measured physical properties of the ceramic are determined by the oxidised layers of the granules on the semiconducting granule, and not by the second vitreous phase.

In the ferroelectric $BaTiO_3$, impurities (Bi, Zr) enrich the surface of the granules; the formation of a ferroelectric domain structure is suppressed in the granules, apparently as a result of the distortion of the $BaTiO_3$ lattice taking place on solution of the impurities.[70]

The development of methods for analysing a surface has made it possible to obtain direct experimental proof of the decisive role of surface structures in the production of various materials: ceramics for electronics,[71] electrode materials for fuel cells,[72] electrodes for the photolysis of water,[73] and semiconducting materials for devices with a Schottky diode.[74]

—o0o—

Thus the study of the formation of surface microstructures and their influence on physicochemical processes in solids is an important research field. The nature of the influence of small quantities of impurity on the properties of a matrix is not completely clear, and contradictory explanations of the observed phenomena have been published. Theoretical studies are required in this field. The methods of physicochemical analysis used at present do not give exhaustive information on the properties of surface microstructures, so that it is necessary to improve further the methods for the quantitative analysis of the chemical composition, the determination

REFERENCES

1. S.J.B.Reed, "Electron Probe Microanalysis" (Translated into Russian), Izd.Mir, Moscow, 1979, 423 pp.
2. P.F.Bongers and P.E.C.Franken, Adv.in Cer., 1981, **1**, 38.
3. V.T.Cherepin and M.A.Vasil'ev, "Metody i Pribory dlya Analiza Poverkhnosti Materialov" (Methods and Instruments for Analysing the Surface of Materials), Izd.Naukova Dumka, Kiev, 1982, 398 pp.
4. C.B.Carter and S.L.Sass, J.Amer.Cer.Soc., 1981, **64**(6), 335.
5. R.W.Carpenter, "Analytical Electron Microscopy and Materials Science, in Preparation and Characterisation of Materials", Eds.J.M.Honig and C.N.R.Rao, Acad.Press, New York, 1981, p.133.
6. B.A.Bender, D.B.Williams, and M.R.Notis, J.Amer.Cer.Soc., 1980, **63**(3–4), 149.
7. S.Z.Bokshtein, S.S.Ginzburg, S.T.Kishkin, and I.M.Razumovskii, Poverkhnost', 1984(1), 5.
8. H.W.Werner and R.P.H.Garten, Rep.on Progr.in Phys., 1984, **47**(3), 221.
9. A.I.Leonov, Yu.P.Kostikov, and L.A.Aksenova, Poverkhnost', 1982(7), 79.
10. A.I.Leonov, Yu.P.Kostikov, E.M.Trusova, et al., Izv.Akad. Nauk SSSR, Neorg.Materialy, 1978, **14**, 498.
11. W.D.Kingery, W.L.Robbins, A.F.Henriksen, and C.E.Johnson, J.Amer.Cer.Soc., 1976, **59**(5–6), 239.
12. W.C.Johnson and D.F.Stein, J.Amer.Cer.Soc., 1975, **58**(11–12), 485.
13. A.I.Leonov, "Vysokotemperaturnaya Khimiya Koslorodnykh Soedinenii Tseriya" (The High-Temperature Chemistry of Oxygen Compounds of Cerium), Izd.Nauka, Leningrad, 1970, p.71.
14. A.I.Leonov, Yu.P.Kostikov, N.S.Andreeva, and E.M.Trusova, Steklo i Keramika, 1979(9), 18.
15. A.I.Leonov, Yu.P.Kostikov, E.M.Trusova, and N.S.Andreeva, Steklo i Keramika, 1979(12), 15.
16. A.I.Leonov, Yu.P.Kostikov, E.M.Trusova, and N.S.Andreeva, Steklo i Keramika, 1979(4), 20.
17. E.G.Keler and N.A.Godina, Ogneupory, 1953(9), 416.
18. A.I.Leonov, Yu.P.Kostikov, I.K.Ivanov, et al., Izv.Akad.Nauk SSSR, Neorg.Materialy, 1979, **15**(11), 1974.

19. A.I.Leonov, Yu.P.Kostikov, I.K.Ivanov, et al., Izv.Akad.Nauk SSSR, 1980, **16**(9), 1576.
20. A.I.Leonov and Yu.P.Kostikov, Zhur.Fiz.Khim., 1982, **56**, 1413 [Russ.J.Phys.Chem., 1982(6)].
21. A.I.Leonov, E.M.Trusova, and N.S.Andreeva, "Termodinamika i Svoistva Kondensirovannykh Silikatov i Okisnykh Sistem" (The Thermodynamics and Properties of Condensed Silicates and Oxide Systems), Veda, Slovatskaya AN, Bratislava, 1976, p.102.
22. Ya.S.Rubinchik, "Soedineniya Okislov Redkozemel'nykh Elementov" (Compounds of Lanthanide Oxides), Izd.Nauka i Tekhnika, Minsk, 1974, p.37.
23. A.I.Leonov, L.A.Aksenova, and Yu.P.Kostikov, "Tezisy Dokladov III Vsesoyuznogo Soveshchaniya po Khimii Tverdogo Tela" (Summaries of Papers Presented at the Third All Union Conference on Solid State Chemistry), Vol.3, Izd.UNTs Akad. Nauk SSSR, Sverdlovsk, 1981, p.24.
24. A.I.Leonov, L.A.Aksenova, N.S.Andrushchenko, et al., Dokl. Akad.Nauk SSSR, Ser.Khim., 1976, **227**, 887.
25. M.A.Kvantov, Yu.P.Kostikov, and A.I.Leonov, Izv.Akad. Nauk SSSR, Neorg.Materialy, 1982, **18**, 1049.
26. J.T.Nowotny and I.Sikora, J.Amer.Cer.Soc., 1982, **65**(4), 192.
27. "Handbook of X-ray Photoelectron Spectroscopy", Ed.G.E.Muilenberg, Perkin Elmer Corporation, Physical Electronics Division, Minnesota, 1979, p.190.
28. D.J.M.Bevan, W.W.Barker, and T.C.Parks, "Rare Earth Research", Gordon and Breach, New York, 1965, **3**, p.467.
29. I.A.Toropov, V.P.Barzakovskii, V.V.Lapin, and N.N.Kurtseva, "Diagrammy Sostoyaniya Silikatnykh Sistem" (The Equilibrium Diagrmas of Silicate Systems), Izd.Nauka, Leningrad, 1969, 821 pp.
30. A.I.Leonov and Yu.P.Kostikov, Poverkhnost', 1983(5), 84.
31. V.S.Stubican and D.Viechnicki, J.Appl.Phys., 1966, **37**, 2751.
32. W.D.Kingery, J.Amer.Cer.Soc., 1974, **57**(1), 1.
33. W. D.Kingery, J.Amer.Cer.Soc., 1974, **57**(1), 1.
34. P.P.Budnikov and A.M.Girtling, "Reaktsii v Smesyakh Tverdykh Veshchestv" (Reactions in Mixtures of Solids), Stroiizdat, Moscow, 1971, 486 pp.
35. Yu.D.Tret'yakov, "Tverdofaznye Reaktsii" (Solid-Phase Reactions), Izd.Khimiya, Moscow, 1978, p.135.
36. E.K.Keler and N.B.Karpenko, Zhur.Neorg.Khim., 1959, **4**, 1125 [Russ.J.Inorg.Chem., 1959(5)].
37. V.B.Glushkova, L.P.Kachalova, V.A.Krzhizhanovskaya, and A.K.Kuznetsov, "Vysokotemperaturnaya Khimiya Silikatov i Oksidov" (The High-Temperature Chemistry of Silicates and Oxides), Izd.Nauka, Leningrad, 1982, p.187.
38. M.G.Osmolovskii, I.K.Ivanov, and Yu.P.Kostikov, Izv.Akad. Nauk SSSR, Neorg.Materialy, 1979, **15**, 118.
39. A.I.Leonov, "Soveshchanie po Kinetike i Mekhanizmu Khimicheskikh Reaktsii v Tverdom Tele" (Conference on the Kinetics and Mechanism of Chemical Reactions in Solids), Izd. IFKhIMS SO Akad.Nauk SSSR, Novosibirsk, Part 1, 1977, p.82.
40. P.D.Ownby and G.E.Junguist, J.Amer.Cer.Soc., 1972, **55**(10), 433.
41. J.M.Neve and R.L.Coble, J.Amer.Cer.Soc., 1974, **57**(6), 274.
42. H.U.Anderson, J.Amer.Cer.Soc., 1974, **57**(1), 34.
43. H.C.Graham and H.H.Davis, J.Amer.Cer.Soc., 1971, **54**(2), 89.
44. A.I.Leonov, Izv.Akad.Nauk SSSR, Neorg.Materialy, 1966, **2**(12), 2168.
45. A.I.Leonov, E.M.Trusova, and N.S.Sadikova, 1974, **10**, 71.
46. E.S.Makarov, "Izomorfizm Atomov v Kristallakh" (The Isomorphism of Atoms in Crystals), Atomizdat, Moscow, 1973, p.107.
47. A.I.Leonov, E.I.Kozlovskaya, and E.K.Keler, Izv.Akad.Nauk SSSR, Neorg.Materialy, 1975, **11**, 2042.
48. A.I.Leonov, E.I.Kozlovskaya, and E.K.Keler, Izv.Akad.Nauk SSSR, 1977, **13**(9), 1640.
49. Y.Wu and G.Reinaecker, Z.anorg.Chem., 1965, **340**, 97.
50. C.R.Manning and L.D.Lineback, "Surfaces and Interfaces Glass and Ceramics", Elsevier, Amsterdam–New York–London, 1974, p.473.
51. A.R.Ubbelohde, "Melting and Crystal Structure" (Translated into Russian), Izd.Mir, Moscow, 1969, p.315.
52. J.Takahashi, I.Yamai, and H.Saito, J.Cer.Soc.Japan, 1975, **83**, 363.
53. N.G.Eror and U.Balachandran, J.Solid State Chem., 1982, **43**, 196.
54. S.B.Desu and E.C.Subbarao, J.Mater.Sci., 1980, **15**(8), 2113.
55. E.C.Subbarao, Bull.Mater.Sci., 1981, **3**, 169.
56. A.I.Leonov, L.A.Aksenova, N.S.Andrushchenko, et al., Izv. Akad.Nauk SSSR, Neorg.Materialy, 1976, **12**, 302.
57. A.I.Leonov, Yu.P.Kostikov, B.A.Rotenberg, and V.S.Strykanov, "Tezisy Dokladov VIII Vsesoyuznoi Konferentsii po Lokal'nym Rentgenospektral'nym Issledovaniyam i ikh Primeneniyu" (Summaries of Papers Presented at the Eight All Union Conference on Local X-Ray Spectral Studies and Their Application), Izd.OIKhF Akad.Nauk SSSR, Chernogolovka, 1982, p.202.
58. M.A.Kvantov, Yu.P.Kostikov, and A.I.Leonov, Izv.Akad. Nauk SSSR, Neorg.Materialy, 1982, **18**, 1049.
59. A.Casalot, O.Monnereau, and M.Drillon, Mater.Res.Bull., 1977, **12**, 861.
60. M.F.Yan and W.W.Rhodes, Appl.Phys.Lett., 1982, **40**, 536.
61. E.I.Leonov, M.A.Kvantov, and Yu.P.Kostikov, Izv.Akad. Nauk SSSR, Neorg.Materialy, 1983, **19**, 799.
62. E.I.Gindin, M.A.Kvantov, Yu.P.Kostikov, and A.I.Leonov, Izv.Akad.Nauk SSSR, Neorg.Materialy, 1983, **19**, 1718.
63. B.B.Leikina, Yu.P.Kostikov, G.N.Tekster-Proskuryakova, et al., Izv.Akad.Nauk SSSR, Neorg.Materialy, 1981, **17**, 1852.
64. M.A.Kvantov and Yu.P.Kostikov, Izv.Akad.Nauk SSSR, Neorg.Materialy, 1980, **16**, 328.
65. W.D.Kingery, J.B.van der Sande, and T.Mitamura, J.Amer. Cer.Soc., 1979, **62**, 221.
66. J.M.Driear, J.P.Guertin, T.O.Sokoly, and L.B.Hackney, Adv.in Cer., 1981, **1**, 316.
67. H.D.Park and D.A.Payne, Adv.in Cer., 1981, **1**, 147.
68. R.Wernicke, Adv.in Cer., 1981, **1**, 261.
69. P.F.Bongers and P.E.C.Franken, Adv.in Cer., 1981, **1**, 38.
70. M.L.Mecartney, R.Sinclair, and G.J.Ewell, Adv.in Cer., 1981, **1**, 207.
71. W.D.Kingery, Adv.in Cer., 1981, **1**, 1.
72. R.N.Singh and N.Lewis, Solid State Ionics, 1983, **9–10**, Pt.1, 159.
73. P.Salvador and C.Guttierrez, Surf.Sci., 1983, **124**(2–3), 398.
74. T.Chot, Phys.Status Solidi, 1982, **70**, 311.

Grebenshchikov Institute of
Silicate Chemistry, Academy of
Sciences of the USSR,
Leningrad